The Journal of Experimental Biology 203, 1539–1550 (2000)
Printed in Great Britain © The Company of Biologists Limited 2000
JEB2547

DYNAMIC MECHANICAL CHARACTERIZATION OF A MUTABLE COLLAGENOUS TISSUE: RESPONSE OF SEA CUCUMBER DERMIS TO CELL LYSIS AND DERMAL EXTRACTS

GREG K. SZULGIT AND ROBERT E. SHADWICK*
Marine Biology Division, Scripps Institution of Oceanography, La Jolla, CA 92093-0202, USA
*Author for correspondence (e-mail: rshadwick@ucsd.edu)

Accepted 28 February; published on WWW 18 April 2000

Summary

The dermis of the holothurian *Cucumaria frondosa* is a mutable collagenous tissue (MCT). In this study, the inner and outer regions of the dermis were separated and used to make two different tissue extracts. These extracts were applied to intact pieces of dermis, one invoking a stiff mechanical state and the other invoking a compliant state. The extracts were effective on tissues incubated in artificial sea water (ASW) and in those incubated in Ca^{2+}-chelated ASW. Furthermore, the extracts were effective on both fresh tissues and tissues in which the cells had been lysed by freeze–thawing, indicating that the sites of action are in the extracellular matrix. Dynamic oscillatory shear tests and analyses were used to measure both the dynamic shear stiffness (G^*) and the relative damping (tanδ) of the tissue. These two parameters proved to be inversely related to each other (i.e. when G^* increased, tanδ decreased). A theoretical viscoelastic model is constructed to interpret the results of these tests. It is concluded that changes in the mechanical state of the tissue involve interactions between elastic elements within the tissue rather than an alteration of its viscous components.

Key words: mutable, connective tissue, collagen, echinoderm, *Cucumaria frondosa*, catch, biomechanics, sea cucumber.

Introduction

Echinoderms share the unique and fascinating ability to alter, rapidly and reversibly, the stiffness of their collagenous connective tissues, commonly referred to as ‘mutable connective tissues’ (MCTs). The mechanism for this neurally mediated change is not well understood, but there are currently several competing models (for a review, see Wilkie, 1996). One of these models proposes that extracellular Ca^{2+} directly controls the stiffness of the tissue, while another suggests that one or more non-ionic substances are released from cells to influence the tissue stiffness. In this study, we test these models as they apply to the dermis of the sea cucumber *Cucumaria frondosa* by chelating extracellular Ca^{2+} and by lysing cells suspected of containing mechano-effective substances. In addition, we use a specifically designed dynamic mechanical test to determine the nature of the extracellular mechanism for this stiffness control. Any knowledge that can be gained about this extracellular mechanism is important because it can help to focus future biochemical work on the appropriate components of the dermis.

Composition of the dermis

Examination of the dermal tissue of the holothurian *C. frondosa* has shown that it follows the pattern of many other MCTs. It is composed of collagen molecules aggregated into bipolar, spindle-shaped fibrils 39–436 μm long (Trotter et al., 1994, 1998) and that have proteoglycans associated with their surfaces (Scott, 1988, 1991; Trotter et al., 1995). Parallel bundles of such fibrils constitute larger structures known as fibers, which are loosely arranged, appearing as a feltwork pattern under the microscope. There is also an extensive, non-collagenous microfibrillar network that permeates the dermis (Thurmond and Trotter, 1996) and may be very important in the mechanical behavior of the tissue. All these components and a sparse assortment of cells, including nerves, reside in an apparently amorphous extracellular matrix that is free of calcareous ossicles (Trotter et al., 1997).

Potential stiffening mechanisms

There are different ideas in the literature regarding the mechanism of MCT stiffening (see Wilkie, 1996). One of these regards Ca^{2+} as the extracellular matrix effector of the stiff state (first proposed by Wilkie, 1978). This idea persists because bathing an MCT in a Ca^{2+}-chelating solution often reduces tissue stiffness (Wilkie, 1978, 1984; Smith et al., 1981; Hidaka and Takahashi, 1983; Diab and Gilly, 1984; Motokawa, 1984b, 1988, 1994; Motokawa and Hayashi, 1987; Shadwick and Pollock, 1988; Wilkie and Emson, 1988), and because adding high concentrations of Ca^{2+} to many tissues (even specimens that have had their cells lysed) results in stiffening (Eylers, 1982; Motokawa, 1984b; Eylers and

Greenberg, 1988, 1989; Kariya et al., 1990). However, MCTs often become stiff, even in the presence of a Ca^{2+}-chelating solution, once their resident cells are lysed (by detergent treatment in Szulgit and Shadwick, 1994; by detergent treatment, freeze–thawing and osmotic shock in Trotter and Koob, 1995; and by freeze–thawing in Koob-Emunds et al., 1996, 1998; but conflicting evidence for the detergent effect has also been found by Motokawa, 1994). On balance, this evidence implies that a tissue-stiffening substance other than Ca^{2+} is being released from the cells.

The Ca^{2+}-independent stiffening of these MCTs has led to a search for mechano-effective substances within the dermis that might play a role in mutability *in vivo*. The holothurian *C. frondosa* has proved to be an excellent subject for this purpose. Koob-Emunds et al. (1996, 1998) and Koob et al. (1999) discovered that, simply by freezing and thawing the entire dermis of this species, they could cause the inner (light) part of the dermis to become quite stiff while the outer (dark) part of the dermis became very compliant. This led them to suspect that there are two separate mechanical effectors in the dermis: one for stiffening, located primarily in the inner dermis, and a second for softening, located primarily in the outer dermis. Because these effects are readily apparent after freezing and thawing, the effectors are thought to be released from lysed cells. They then showed using 'bend tests' that certain isolated components are mechanically effective, while others are not. In the present study, we reproduce the crude extracts of the inner and outer dermis discussed in Koob-Emunds et al. (1996, 1998) and Koob et al. (1999) and apply them to both non-frozen and freeze–thawed pieces of dermis, in the presence and absence of a Ca^{2+} chelator, to determine more specifically their effects on the extracellular portion of the tissue.

How best to test the mechanical state of the tissue?

There have been many mechanical investigations of holothurian dermis over the last 20 years (for a review, see Wilkie, 1996). The experimental methods in these studies have focused on mechanical tests such as creep, stress relaxation and stress/strain tests. While these tests have shed some light on the mechanism of mechanical mutability, they are intrinsically limited in the number of parameters that they can explore quickly and accurately. Many substances exhibit time-dependent properties that can be found through these tests, but MCTs are known to show further changes in their properties as a result of the testing procedures themselves (Shibayama et al., 1994; present study). This means that a calculated 'constant' can change from test to test for the same specimen. Using only these tests, therefore, it is difficult to characterize mechanically a given MCT. Dynamic oscillatory tests, in contrast, provide an extra dimension of analysis by monitoring the effects of the testing procedure itself. They therefore provide a more complete characterization of the stiff and compliant states of the tissue. We have employed testing methods that were developed by polymer engineers to study viscoelastic substances over broad ranges of frequencies but, because *C. frondosa* dermis rapidly changes its mechanical properties as a result of testing, we modified these techniques to analyze the tissue at only one frequency.

Viscoelasticity is a concept that is commonly referred to in the quantitative description of polymers. It is derived from the terms 'viscosity' (which can be thought of as 'molecular friction' and is responsible for the rate of flow of a fluid and for non-recoverable dissipation of strain energy in response to an applied force) and 'elasticity' (which is responsible for the portion of energy that can be recovered from deformation caused by an applied force). The term 'viscoelastic', therefore, describes materials with elastic properties that are dependent upon the rates of extension of the materials. In truth, all materials exhibit some degree of viscoelasticity, but the term is best exemplified by materials such as those composed of long-chain polymers (e.g. natural, unprocessed rubber) whose combination of viscosity and elasticity is readily apparent.

In the compliant state of the sea cucumber dermis, the fibrils apparently slide past each other easily (Trotter and Koob, 1995). Conversely, in the stiff state, the fibrils are prevented from sliding past each other. If the tissue is modeled as a composite of discontinuous elastic fibrils in a viscous solution (Harris, 1980), two general mechanisms can easily be imagined for its stiffening: one relying on viscous factors and one relying on elastic factors. These general mechanisms can reflect what is going on inside the tissue at the molecular level, provided they are considered in the appropriate context. In this study, the context takes the form of a theoretical viscoelastic model (described in depth in the Discussion section of this paper). This model has elastic and viscous elements that are combined in such a way that the behavior of the entire system mimics the previously established mechanical behavior of *C. frondosa* dermis. This allows us to predict the overall dynamic oscillatory behavior of the tissue under hypothetical conditions. A few of these conditions are considered as possible mechanisms for overall tissue stiffening and are detailed below.

The first hypothetical mechanism (mechanism 1) is as follows: the increase in stiffness is due to an increased contribution from the viscosity of the interfibrillar solution, a conclusion that has been arrived at by others (Eylers, 1982; Motokawa, 1984b; Eylers and Greenberg, 1988, 1989) using different methods from those used in the present study. Collagen fibrils sliding through this solution encounter increased resistance as a result of increased interaction with the surrounding, primarily viscous, solution components (Fig. 1A). The surfaces of these fibrils are known to be non-covalently associated with proteoglycans (Trotter et al., 1995), and interactions between these and the surrounding viscous components undoubtedly affect the amount of force required to drag the fibrils through the surrounding solution. If these interactions were increased by, for example, a change in conformation, charge distribution or charge shielding, then one might expect an increase in tissue stiffness resulting from an increased reliance on viscosity as opposed to elasticity.

The second hypothetical mechanism (mechanism 2) is as follows: the increase in stiffness is due to an increased

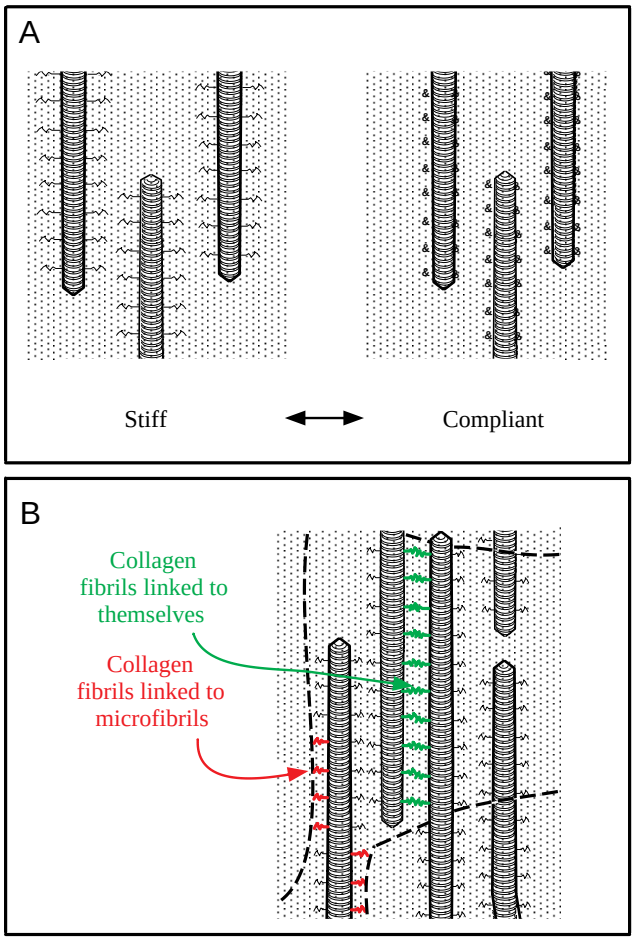

Fig. 1. Hypothetical mechanisms for dermal stiffening. (A) Mechanism 1: stiffness is altered by changing the interactions between the surfaces of the fibrils and the primarily viscous interfibrillar solution. (B) Mechanism 2: stiffness is altered by changing the interactions between the fibrils and themselves or other elastically dominated components of the dermis, particularly the microfibrils.

contribution from the elastic components. This could be due to adjacent fibrils becoming linked together by ionic forces, by microfibrils interacting with the fibrils or by some other mechanism (Fig. 1B). If the tissue is modeled as a pliant composite of fibrils within a viscous solution, then the force transferred through the solution to the fibrils depends on the size and orientation of the fibrils or fibrillar aggregates (Harris, 1980). If two or more fibrils became linked, then their effective size would increase and they would be subject to a greater proportion of the load on the tissue. Assuming that these fibrillar aggregates partially account for the elastic nature of the tissue, one would expect that an increase in their size would lead to an increased contribution on their part towards stiffening the tissue. Furthermore, if some of these fibrils linked together to form a tissue-spanning network, then the elastic contribution to tissue stiffness would increase dramatically.

The two general hypothetical mechanisms can be distinguished from each other by dynamic mechanical tests on large pieces of intact tissue to determine which of the two predicted modes of action occurs when the tissue changes its stiffness. If mechanism 2 is favored, then we should also be able to determine whether the elastic elements involved span the tissue. Further details as to which molecular components are responsible for stiffening cannot be elucidated without a greater knowledge of tissue composition.

Materials and methods

Obtaining and preparing tissue specimens

Sea cucumbers [*Cucumaria frondosa* (Gunner)] of medium size (335±66 g wet mass) were collected off the coast of Maine and shipped overnight to California. They were kept in a flow-through seawater aquarium at 9 °C, where they were allowed to acclimate for at least 3 days prior to testing. To maintain normal cellular functions, no drugs were administered. To obtain standard tissue specimens, each individual was induced to become stiff by gently drumming on its surface with a few fingers prior to cutting (this is necessary to ensure a well-defined, smooth tissue surface after cutting). It was then split longitudinally along the ventral surface using a razor blade so that the viscera and muscle layers on the inside of the body wall could be removed using forceps, leaving only the collagenous dermis. Razor blades, held in parallel with constant spacing in special holders, were then used to cut standard-sized tissue pieces from the central dorsal area of the dermis as follows: the dermis was cut through radially, creating several wafers that were then turned on their sides, allowing the circumferential cuts that separated the inner from the outer dermis (a distinction that was determined visually). These specimens measured 12±1 mm×1.8±1.0 mm×2.3±0.5 mm (means ± S.D., N=30, corresponding, respectively, to the longitudinal, radial and circumferential axes of the sea cucumber, and included only tissue from the inner dermis (the light region of the dermis).

We also generated an equal number of specimens that included both the inner and the outer dermis (the light and the dark regions), which were similar in all other respects except that they were 3.8±1.1 mm in the radial axis. All experiments performed on the inner dermis specimens were also performed on the whole dermis (inner and outer dermis) specimens. The data for experiments with whole dermis are not reported in this paper, but are briefly discussed with the other results.

Bathing media

Many of the tests required that the tissues be exposed to sequential bathing solutions. Tissues transferred between media baths were first briefly rinsed in the next medium to reduce contamination between media baths. Tissues were exposed to each bathing medium by placing 4–8 specimens in a small beaker containing 35 ml of medium, which was shaken gently at 4 °C to keep the medium slightly stirred. All media baths had corresponding control baths of equivalent volume containing the same number of specimens.

Media consisted of artificial sea water (ASW; of the following composition: 445 mmol l^{-1} NaCl, 60 mmol l^{-1} $MgCl_2$, 10 mmol l^{-1} KCl, 2.4 mmol l^{-1} $NaHCO_3$, 10 mmol l^{-1} Hepes and either 10 mmol l^{-1} $CaCl_2$ or 2.5 mmol l^{-1} EGTA to make the Ca^{2+}-chelating solution; pH 7.8 in each case) that had tissue extracts added to it for certain specified tests. Extracts were freshly prepared for each individual from the remainder of the dermis that was not used for testing. This tissue was freeze–thawed (see below) once to make the inner and outer dermis easily separable from each other. Once these two regions had been separated, they were finely minced with a razor blade and placed in separate ASW or Ca^{2+}-chelated ASW media. These solutions were then further freeze–thawed twice to ensure cell lysis, stirring the solution after each thaw. These solutions will be referred to hereafter as IDE (inner dermis extract) and ODE (outer dermis extract).

Tissue freeze–thawing (cell lysis of the test specimens)

Tissues were frozen by placing the beaker containing the bathing medium and the tissues into a shallow slurry of dry ice and methanol. The medium was frozen until it became bright white in color (note that freezing the medium at a higher temperature, e.g. –20 °C, is not adequate). Each speciman was then thawed by floating the beaker in warm tapwater until the medium was nearly thawed, and then allowing it to thaw on a dry desktop at room temperature. Tissue specimens were kept refrigerated until just prior to testing, at which point they were allowed to reach room temperature (19–26 °C). All controls were treated in a similar manner.

Testing methods

Tissue specimens were placed between two parallel glass slides that had pieces of waterproof sandpaper attached to them with epoxy adhesive, and the slides were brought together to a standard distance of 2.3 mm (Fig. 2). A periodic voltage was generated by a Rockland System/90 signal analysis workstation and delivered to an electromagnetic vibrator (model 400, Ling Dynamic Systems) *via* a power amplifier. This drove the top slide at a frequency of 1 Hz (chosen arbitrarily) in a sinusoidal oscillatory fashion, shearing the tissue longitudinally at a strain of ±3 % (±0.07 mm). Displacement of the top slide was measured by a linear variable differential transformer (LVDT), while force was measured by a strain gauge set on a double-bending beam transducer attached to the bottom slide. The force transducer was magnetically attached to a massive steel table that rested in a box of sand to isolate the force transducer from background mechanical vibrations. The oscillatory driver and upper glass plate were securely fastened to a separate table (Fig. 2). All specimens were kept moist and tested at room temperature.

Force and displacement were measured, and the signals were conditioned by matched amplifiers before being recorded digitally using an Axon Instruments TL-2 interface board and Axotape 1.3.0.09 software on a 386-PC. Dynamic shear stress and strain values were derived from force and displacement measurements. Often, and most notably in the tests with the Ca^{2+}-chelated specimens, each tissue started out with a certain stiffness only to become rapidly much less stiff (commonly 2–5 times less stiff in Ca^{2+}-chelated specimens) as the tissue specimen was sheared (Fig. 3) (i.e. the amplitude of the force measurements decreased while the amplitude of the displacement measurements remained constant). To avoid the pitfalls associated with analyzing non-steady (non-stationary) data, only the last eight cycles of each 50-cycle test (at 1 Hz), by which time the amplitudes of the cycles had become relatively uniform, were compared to calculate viscoelastic parameters (Fig. 3).

Dynamic measurements of mechanical properties

Because *C. frondosa* dermis is viscoelastic, the maximum oscillatory shear displacement lagged behind the maximum oscillatory force transmitted through the material by an amount that will be referred to as δ (the 'phase lag'; see Fig. 2).

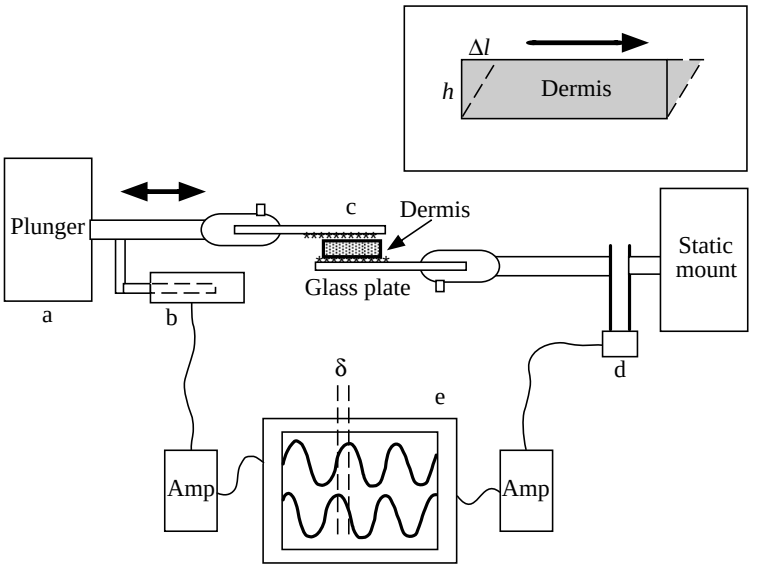

Fig. 2. The dynamic oscillatory shear device. An electromagnetic plunger (a) is driven in a smooth, sinusoidal fashion at 1.0 Hz, and its displacement is measured with a linear variable differential transformer (b). Specimens are placed between the gripping surfaces of two glass plates (c), which are brought together to a known proximity. A force transducer (d) is attached to the bottom plate. Displacement and force signals are recorded and compared (e). Inset: schematic view of the tissue specimen being sheared. Dynamic shear stiffness (or complex shear modulus; G^*) is an expression of the maximum oscillatory shear stress (force/area) and shear strain (change in length/height) at the small strain values used in this study. h, height of tissue specimen; Δl, change in the length of the specimen; δ, phase lag.

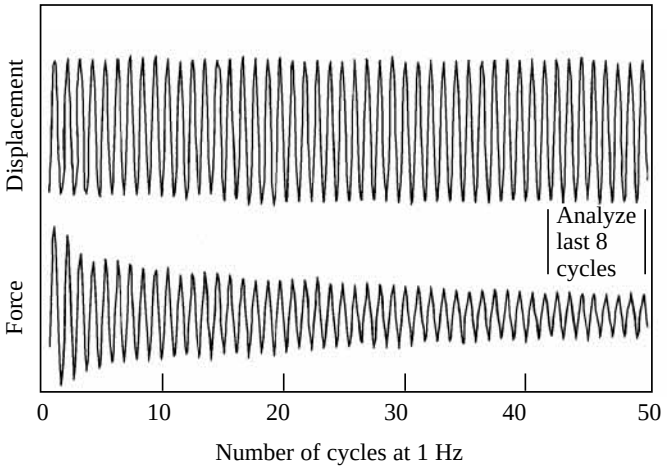

Fig. 3. Typical displacement and force data for a freeze–thawed, Ca^{2+}-chelated tissue specimen of *Cucumaria frondosa*. These data are meant to show that the force decreases exponentially with testing, but that it is uniform for the last eight cycles (those used for analysis in each data set). Scale bars are not included because, while maximum displacement was kept constant (±0.07 mm) for each specimen, the forces transmitted through the specimens differed dramatically.

Sinusoidal force and displacement signals were measured simultaneously, and this data set was resolved into G^* (the dynamic shear stiffness or complex shear modulus) and tanδ (the 'damping', which is the ratio of the loss modulus to the storage modulus) by using the following relationships (Ward, 1983).

In oscillatory shear tests, the shear strain (γ) and shear stress (τ) are expressed as functions of time (t) by:

$$\gamma_{(t)} = \gamma_o \sin(\omega t), \quad (1)$$

and

$$\tau_{(t)} = \tau_o \sin(\omega t + \delta), \quad (2)$$

where γ_o is strain amplitude, τ_o is stress amplitude, ω is circular frequency and δ is the phase lag.

The dynamic oscillatory shear stiffness is:

$$G^* = \tau_o/\gamma_o, \quad (3)$$

which allows equation 2 to be written as:

$$\tau_{(t)} = \gamma_o G^* \sin(\omega t + \delta) \quad (4)$$

or, by trigonometric identity, as:

$$\tau_{(t)} = \gamma_o(G^*\cos\delta)\sin(\omega t) + \gamma_o(G^*\sin\delta)\cos(\omega t), \quad (5)$$

indicating that there is a component ($G^*\cos\delta$) of τ that is in phase with strain [sin(ωt)] and another component ($G^*\sin\delta$) of τ that is in phase with strain rate [cos(ωt)]. The term $G^*\cos\delta$ is the storage modulus (G') and represents the elastic contribution to stiffness. The term $G^*\sin\delta$ is the loss modulus (G'') and represents the viscous contribution to stiffness. The dynamic shear stiffness (also called the complex shear modulus) (G^*) can, therefore, be represented as a vector resultant of the in-phase and out-of-phase components

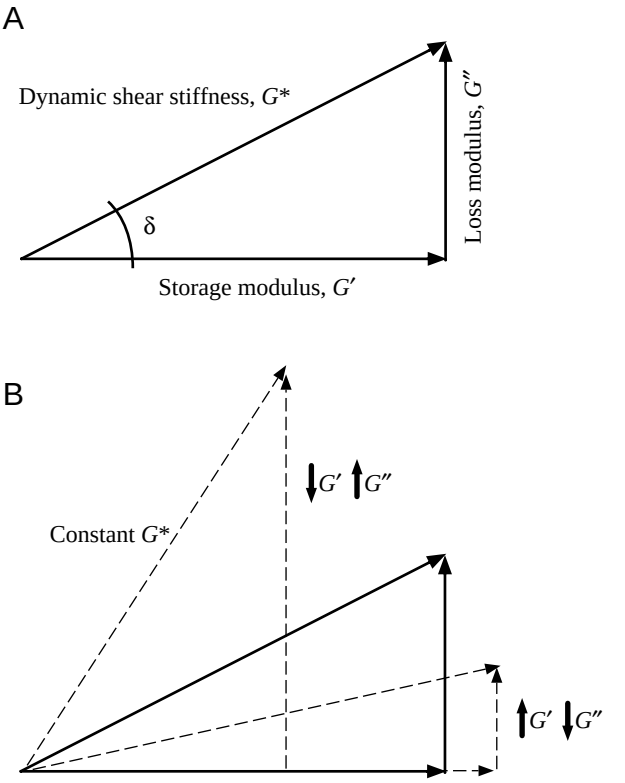

Fig. 4. Vector diagrams of the relationships between moduli. (A) The storage modulus (G') represents the elastic contribution to stiffness, while the loss modulus (G'') represents the viscous contribution to stiffness. The dynamic shear stiffness or complex shear modulus (G^*) can, therefore, be represented as a vector resultant of the two, and their ratio can be expressed as tanδ. (B) Note that G^* is independent of tanδ if G' and G'' are allowed to change independently. In the example shown here, changing G' and G'' causes G^* to remain the same even though tanδ changes. Alternatively, changing G' and G'' in the same direction and in proportion would cause G^* to change while tanδ remained the same.

(Fig. 4A). Note that the same value for G^* can be arrived at by more than one combination of G' and G'' (Fig. 4B) (Ward, 1983).

These terms are useful in expressing the relationships between certain material properties. The tangent of δ describes the ratio of the loss to the storage modulus:

$$\tan\delta = G''/G'. \quad (6)$$

Plotting tanδ *versus* G^* therefore expresses how G' and G'' change with respect to dynamic shear stiffness. Note that tanδ is independent of G^*, so the two parameters are not self-referencing when plotted against each other.

Experiments were designed to compare values within individuals and not among animals because MCTs are notorious for having highly variable mechanical properties between individuals (G. K. Szulgit and R. E. Shadwick, personal observations; T. Motokawa, R. Birenheide, J. Trotter and F. Thurmond, personal communication). Data were analyzed by spectral analysis (fast Fourier transform of each

series calculated in polar form compared as ratios) using DADiSP ver2.0 from DSP Development Corporation and Quatro Pro ver3.0 from Borland; statistical tests were performed using Super ANOVA from Abacus Concepts; and theoretical viscoelastic modeling was performed with the aid of Working Model ver2.0 from Knowledge Revolution.

Results

The results of these experiments strongly support the idea that there are at least two different substances in the dermis of *C. frondosa* affecting its stiffness and that these substances are contained within cells. They also indicate that the induction of the stiff and compliant states does not depend on the presence or absence of Ca^{2+}. A quantitative analysis (Table 1) shows that the mean stiffness values for the tissues exposed to IDE were much higher than the mean stiffness values for those exposed to ODE (approximately 20–30 times as high for the non-frozen tissues and approximately 8–15 times as high for the freeze–thawed tissues). There is a noticeable increase in variation at the lower end of the stiffness values (Fig. 5). This may be artifactual because the tissues that were extremely compliant (e.g. G^*<1 kPa) were very difficult to place into the testing apparatus in a uniform fashion that would ensure a precise measurement.

We found that there was no difference between the isolated inner dermis specimens and the whole dermis specimens in any of our tests (data not shown for the whole dermis). The mechanical properties of the outer and inner dermis are quite different, but the outer dermis is so much more compliant than the inner dermis that any force transmission through it was probably overwhelmed by the stronger signal from the inner dermis. The contribution of the outer dermis to tissue stiffness is, therefore, considered to be insignificant.

Non-frozen tissues

The dermis of *C. frondosa* behaved like other holothurian MCTs when non-frozen pieces were incubated in either ASW or Ca^{2+}-chelated ASW (Motokawa, 1981, 1982, 1984a,b, 1994; Eylers, 1982; Hayashi and Motokawa, 1986; Eylers and Greenberg, 1988, 1989; Kariya et al., 1990). Tissues in ASW were generally stiff (in first incubations 70±9.9, 78±14 and 79±14 kPa), while tissues in Ca^{2+}-chelated ASW were comparatively compliant (in first incubations 14±8.6, 8.3±2.5 and 8.5±3.4 kPa) (Fig. 5A). We do not think that the high stiffness in the ASW group was an effect of the ASW solution because the tissues were stiff at the time of dissection (observed by touch and by visual inspection when subjected to gravity as a cantilevered beam). This high initial stiffness seemed to be a direct result of mechanical stimulation prior to cutting and as a result of the dissection itself. The tissues incubated in Ca^{2+}-chelated ASW were approximately an order of magnitude less stiff than those in ASW, which is less compliant than expected, given the results of previous mechanical investigations into MCTs (Motokawa, 1981, 1982, 1984a,b, 1994; Eylers, 1982; Hayashi and Motokawa, 1986; Eylers and Greenberg, 1988, 1989; Kariya et al., 1990). We suspect that the dermis of *C. frondosa* is much less ionically permeable than other MCTs (*P. parvimensis* dermis, for example, was affected by its bathing solutions after only 1 h of incubation, as opposed to the 24 h that it took to see an effect in *C. frondosa* dermis (G. K. Szulgit and R. E. Shadwick, personal observations). Detailed effects of such 24 h incubations on the mineral content of *C. frondosa* dermis have been reported by Trotter et al. (1997). This low permeability may have contributed to the difference in compliance seen between *C. frondosa* and these other MCTs.

After initial testing, each tissue was incubated for 24 h in a control solution or in a solution containing an extract before testing again. During this time, the ASW control tissues (i.e. those maintained continuously in ASW) lost varying amounts of stiffness so that they spanned more than two orders of magnitude in stiffness (range 0.2–50 kPa; Fig. 5B), while the stiffness of the Ca^{2+}-chelated controls did not change significantly (from 8.3±2.5 to 8.3±2 kPa) (Fig. 5C). The

Table 1. *A quantitative analysis of shear stiffness values measured in the inner dermis of* Cucumaria frondosa

First incubation	G^* (kPa)	Second incubation	G^* (kPa)
Non-frozen specimens			
ASW	70±9.9	ASW+ODE	0.92±0.32
	78±14	ASW	9.1±5
	79±14	ASW+IDE	30±19
Ca^{2+}-chelated	14±8.6	Ca^{2+}-chelated+ODE	1.6±1
	8.3±2.5	Ca^{2+}-chelated	8.3±2
	8.5±3.4	Ca^{2+}-chelated+IDE	32±14
Freeze–thawed specimens			
ASW	16±2.2	ASW+ODE	1.3±0.37
	13±2.9	ASW	8.4±4
	16±7.0	ASW+IDE	20±10
Ca^{2+}-chelated	16±4.3	Ca^{2+}-chelated+ODE	2.4±1
	28±13	Ca^{2+}-chelated	24±11
	16±3.1	Ca^{2+}-chelated+IDE	21±3

Comparison of dynamic shear stiffness values (means ± S.E.M.) where each value is an average of four means from four animals.

In the first incubation of each group (Non-frozen and Freeze–thawed), a two-factor analysis of variance (ANOVA) for repeated measures determined that, within each water type (ASW or Ca^{2+}-chelated), none of the main effects caused significant differences between stiffness values (i.e. the first incubations within any water type were statistically similar).

In the second incubation of each group, a two-factor ANOVA for repeated measures determined that, within each original water type (ASW or Ca^{2+}-chelated), the main effect of the extract caused significant differences between stiffness values.

A *post-hoc* test (Bonferroni–Dunn test of all means) showed that, in each case, tissues incubated in ODE solutions were significantly different from those incubated in IDE solutions ($P \leqslant 0.05$).

ASW, artificial sea water; IDE, inner dermis extract; ODE, outer dermis extract; G^*, dynamic shear stiffness.

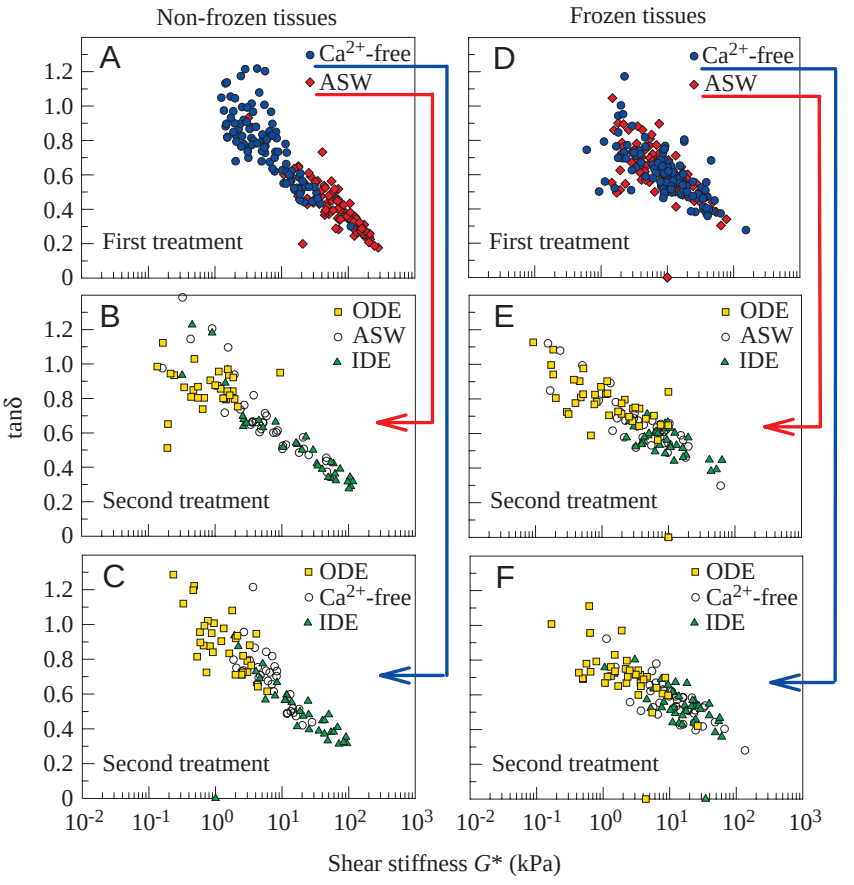

Fig. 5. Dynamic shear stiffness (*G**) *versus* damping (tanδ) for *Cucumaria frondosa* dermis. Mean values ± S.E.M. are given in Table 1. Each point represents the value for one treatment of one tissue specimen. Non-frozen tissues: in the first incubation (A), tissues that were exposed to Ca^{2+} chelation became less stiff than those exposed to artificial sea water (ASW). In the second incubation, ASW-incubated (B) and Ca^{2+}-chelated (C) tissues were both affected similarly in that they were the most stiff in inner dermis extract (IDE) and the least stiff in outer dermis extract (ODE). Freeze–thawed tissues: in the first incubation (D), there was no difference between ASW-incubated and Ca^{2+}-chelated tissues. In the second incubation, ASW-incubated (E) and Ca^{2+}-chelated (F) tissues were both affected similarly in that they were the most stiff in IDE and the least stiff in ODE. See Fig. 4 for an explanation of tanδ.

absence of Ca^{2+} may inhibit a change in the mechanical state of the tissue, but the mechanism for this inhibition is not clear.

Effects of IDE on the non-frozen tissues

Tissues exposed to inner dermis extract tended to be stiffer than their controls (30±19 versus 9.1±5 kPa for the ASW group and 32±14 *versus* 8.3±2 kPa for the Ca^{2+}-chelated group) (Fig. 5B,C). This suggests the presence of a stiffener in the inner dermis that works even in the presence of a Ca^{2+} chelator. Specifically, those tissues that started out fairly compliant (the Ca^{2+}-chelated tissues at 8.5±3.4 kPa) tended to increase in stiffness in the presence of IDE (up to 32±14 kPa), while those that started out stiff (the ASW-pretreated tissues at 79±14 kPa) tended to retain their stiffness (to 30±19 kPa) relative to the other groups.

Effects of ODE on the non-frozen tissues

Tissues exposed to outer dermis extract showed a compliant trend when compared with controls, with no significant difference between the groups incubated in ASW + ODE and Ca^{2+} chelator + ODE (0.92±0.32 *versus* 1.6±1 kPa) (Fig. 5B,C). This suggests the presence of a softener in the outer dermis that works even in the presence of Ca^{2+}.

Freeze–thawed tissues

As discussed above, the IDE and ODE affected the non-frozen tissues, but it is not clear how. The extracts may have affected cells in the non-frozen tissue, which then released mechano-effective factors, or the extracts may have affected the extracellular matrix directly. To distinguish between these possibilities, tissues from four individuals were freeze–thawed to lyse the resident dermal cells prior to incubation (a method shown to be effective by Trotter and Koob (1995) and Szulgit and Shadwick (1998). This should have destroyed the cells in the dermis, causing them to release their contents into the extracellular matrix.

Each tissue specimen was much stiffer after freezing than it had been prior to freezing (observed by touch and by visual inspection when subjected to gravity as a cantilevered beam). Other investigators have also compared these two parameters within individuals and have shown that freeze–thawing stiffens *C. frondosa* inner dermis considerably (Trotter and Koob, 1995). Although the ASW freeze–thawed tissue groups in our study actually had lower mean stiffnesses than their non-frozen counterparts (in first incubations 16±2.2, 13±2.9 and 16±7.0 kPa *versus* 70±9.9, 78±14 and 79±14 kPa), caution needs to be exercised when comparing data across groups (freeze–thawed *versus* non-frozen). Our tests were designed to reveal relative changes within individuals (to eliminate variation among individuals), and the individuals used in the freeze–thaw tests were sent to us in a separate shipment from Maine. They were approximately two-thirds of the size of those used in the non-frozen tissue tests and may have shared other factors that could have affected their absolute, as opposed

to relative, stiffness values. The conclusions in the present study are, therefore, based only on stiffness values in comparison with their appropriate controls.

Freeze–thawing alone seemed adequate to stiffen what would have otherwise been compliant tissues (the Ca^{2+}-chelated tissues were just as stiff after freezing, 28±13 kPa, as the ASW tissues after freezing, 13±2.9 kPa; Fig. 5D). This could be the result of an agent being released from lysed cells in the inner region of the dermis. The next 24 h incubation revealed that the extracts were, indeed, effective directly on the extracellular matrix (Fig. 5E,F). Note that the ASW and Ca^{2+}-chelated control groups tended to retain their stiffness (the stiffness of the ASW group changed from 13±2.9 to 8.4±4 kPa, while that of the Ca^{2+}-chelated group changed from 28±13 to 24±11 kPa).

Effects of IDE on the freeze–thawed tissues

Tissues exposed to inner dermis extract in ASW tended to be stiffer than their controls (20±10 *versus* 8.4±4 kPa), while their Ca^{2+}-chelated counterparts were just as stiff as their control group (21±3 *versus* 24±11 kPa; Fig. 5E,F). It is important to note that the stiffness in this case occurred in the presence of a Ca^{2+} chelator because it argues that the extracted stiffening agent does not consist of free Ca^{2+}.

Effects of ODE on the freeze–thawed tissues

The ODE solutions caused a tendency towards compliance in the tissues (2.4±1 kPa for the Ca^{2+}-chelated group *versus* 24±11 kPa for the control and 1.3±0.37 kPa for the ASW group *versus* 8.4±4 kPa for the control) (Fig. 5E,F). This is important because it shows that the freeze–thaw stiffness is not an artifact (freeze–thawing the tissues in ASW could conceivably damage the proteins or their interactions, creating an artificially stiff state. The fact that the stiff state of the tissues can be easily reversed by the presence of a tissue extract and does so in a manner identical (with regards to tanδ *versus* G^*) to that seen in the non-frozen tissue tests argues strongly against the freeze–thaw stiffness being an artifact). Note that the ODE also works in the presence or absence of Ca^{2+}.

Effects of shear testing on the tissues

Most tissues became more compliant between the beginning and the end of the 50-cycle test. This testing effect was very slight in specimens treated with ASW, but was more pronounced in Ca^{2+}-chelated specimens. This phenomenon occurred in stiff (freeze–thawed) tissues as well as in compliant tissues, which indicates that chelating Ca^{2+} does, indeed, seem to have some direct effect on the extracellular matrix. The effect is not pronounced enough to be responsible for mutability, because the freeze–thawed Ca^{2+}-chelated and IDE-exposed Ca^{2+}-chelated tissues are still quite stiff at the end of the 50-cycle test (remember that the data in Fig. 5 are all taken from the last eight cycles of each 50-cycle test), but it is an enigmatic effect that is worth noting. Ca^{2+} may be acting either on the tissue in a manner that is fundamentally different from that of the extracts or in a similar fashion. It is possible that Ca^{2+} chelation is interfering with viscous interactions (between fibril surface proteoglycans and the surrounding fluid, for example), but it is difficult to explain how this would lead to the reduction in stiffness due to oscillatory shear seen in our tests. It seems more plausible that the reduction in stiffness over the course of each test would be the result of either chemical bonds being broken or components untangling from each other over the course of the tests.

Discussion

Significance of the relationship between stiffness and damping

Although specimens subjected to the range of treatments employed produced a range of stiffness and tanδ values, the inverse relationship between G^* and tanδ remained consistent (Fig. 5). A linear regression through all the data (grouped) is best fitted by the equation:

$$\tan\delta = -0.26\log_{10}G^* + 0.87\,, \qquad (7)$$

where G^* is dynamic shear stiffness (in kPa). The negative slope indicates that, as the tissue stiffness increased, the relative contribution from viscosity decreased. In other words, the mechanical response of the tissue became more elastically dominated (i.e. it became more resilient as it stiffened).

The results of the oscillatory tests on the ASW-treated specimens are critical because they establish a baseline relationship between G^* and tanδ under chemically innocuous conditions (the ionic composition of the ASW-incubated dermis should be nearly the same as that of the freshly dissected dermis; Trotter et al., 1997). The relationship between G^* and tanδ (equation 7) therefore serves as a ‘signature’ for the most physiologically relevant conditions. If a method is employed that does not produce this signature relationship, then we would suspect that the effects are not physiologically relevant.

Our results do not support the model that Ca^{2+} is responsible for stiffening the tissues *in vivo*. Instead, they support the idea that the dermis is stiffened by the release of one or more stored cellular components into the extracellular matrix that are not affected by the introduction of the chelator EGTA. Because the non-frozen tissues treated with Ca^{2+} chelator, the freeze–thawed tissues, the tissues treated in ASW and those treated with the dermis extracts all exhibited the same behavior with regard to the signature relationship between tanδ and G^*, we suggest that these treatments might either invoke or mimic the natural stiffening processes in the tissue specimens.

Choosing and interpreting an appropriate theoretical model

Before one can draw any conclusions regarding the alteration of viscous or elastic elements in the *C. frondosa* dermis, a model must be chosen as a framework for interpreting the data. For this purpose, we constructed theoretical representations of the tissue composed of springs and dashpots. The springs represent linear Hookean elements wherein the stress transmitted through them is proportional to the strain imposed on them. The dashpot is representative of a

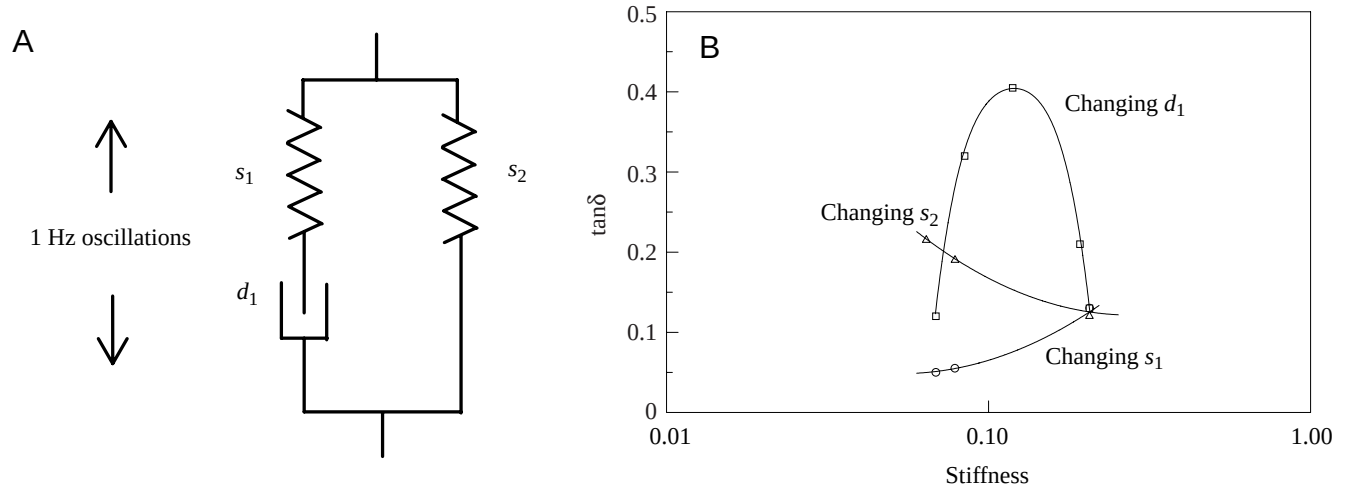

Fig. 6. Viscoelastic model of the tissue (A). The elements represent the categories of tissue components that are necessary to describe accurately the known behavior of the tissue. Each category consists of known and unknown structural components. The spring and dashpot in series (s_1 and d_1, respectively) make up a Maxwell element, which would eventually extend to failure, under any load, if it were not for the parallel spring element (s_2). The behavior of the model is seen (B) when the values of the variables that describe the elements are altered. The line with the positive slope results from changing s_1, that with the negative slope from changing s_2 and the parabolic function from changing d_1. Note that the units on this graph are arbitrary, but that the relative scale is accurate. See Fig. 4 for an explanation of tanδ.

viscous (damping) element, wherein the stress transmitted through it is proportional to the strain rate that is imposed on it. This modeling technique is common practice among polymer engineers and has been employed on several occasions to describe MCTs (Eylers, 1982; Motokawa, 1984b; Eylers and Greenberg, 1988, 1989).

The placement of the elements in our model was critical to its overall behavior and was dictated by the existing empirical data for *C. frondosa* dermis and other MCTs. It is known that MCTs can change both during the course of a test and as a result of that test (Shibayama et al., 1994; present study). Any relaxation time 'constants' that could be calculated will, therefore, actually change throughout the test unless the constant is being calculated from a stable portion of the data set. For this reason, we did not calculate specific time constants for this tissue, but used a range of constants to develop general trends in our model.

The well-established existence of an extensive network of microfibrils that permeates the tissue was considered when creating our model. Because this microfibrillar network recovers elastically to its original length after extension (Thurmond and Trotter, 1996), the tissue cannot be modeled with a terminal dashpot in series with the other elements (the simplest version of which would be commonly referred to as a Maxwell model), but must include a spring in parallel. The fact that *C. frondosa* dermis has been shown to creep to the point of failure under a high enough load (Trotter and Koob, 1995) seems, at first, to argue that microfibrils are not acting as springs in parallel. Upon closer consideration, however, one sees that the load affecting the dermal specimens in the study of Trotter and Koob was so high that the microfibrils must have broken. The constant load that was used caused a stress of 1.21 MPa on the dermal specimens but, as the collagenous fibrils in the creeping tissue slid apart from each other and no longer acted as load-bearing elements, the microfibrils would have been the only elements left to support this load. Because the microfibrillar network accounts for only 3.65 % of the cross-sectional area of the tissue (Thurmond and Trotter, 1996), the stress on the microfibrils would have climbed as high as 33.2 MPa. Such a stress is well in excess of the breaking stress of 14.5 MPa of the isolated microfibrillar network (Thurmond and Trotter, 1996), so a constant stress of 1.21 MPa would result in the microfibrillar network (represented by a parallel spring in our model) creeping to the point of rupture. Assuming that there were no other significant elastic elements spanning the dermal tissues in the study of Trotter and Koob (1995), we would expect the specimens to do the same.

When one considers all the existing mechanical data for *C. frondosa* dermis, the commonly used model for a 'standard linear solid' (Fig. 6A) (Ward, 1983) seems to be the most appropriate to represent this MCT, in spite of the 'non-standard' properties of the tissue. The model contains a spring (s_1, representing collagen fibrils as discontinuous, elastically dominated structures) and a dashpot (d_1, representing the interfibrillar solution and its viscously dominated components) in series. This alignment permits stress relaxation, which has been demonstrated in the MCTs of sea cucumbers (Eylers, 1982; Motokawa, 1984b; Eylers and Greenberg, 1988, 1989). The model also has a spring (s_2, representing a continuous, primarily elastic network) in parallel, preventing creep to the point of failure. In the most compliant tissue state, s_2 represents the properties of a stable microfibrillar network shown by Thurmond and Trotter (1996). If the spring constants and/or the viscosity of the dashpot are altered, the model produces a mechanical response that can be compared with that observed

in the oscillatory tissue tests to give some clues as to how the tissue is changing under certain situations.

Looking at the model-generated data (Fig. 6B), one can see that changing the spring constant for s_1 gives results that have a positive slope when tanδ is plotted against G^* (i.e. tanδ increases as G^* increases). This is the opposite of the empirical result seen when stiffness is induced by tissue extracts. Changing the spring constant for s_2, however, gives a negative slope when tanδ is plotted against G^* (i.e. tanδ decreases when G^* increases). This behavior is more similar to that seen when the tissue changes as a result of exposure to extracts, freeze–thawing or manipulation of $[Ca^{2+}]$ when the cells in the tissue are intact. This result suggests that the phenomenon of mutability is due to an increased reliance on, or alteration of, the elastic elements that span the tissue (i.e. s_2), which could occur if the sliding collagen fibrils were to become linked into a network. Including collagen fibrils in a network implies that they are no longer discontinuous, effectively 'switching' them over from the s_1 to the s_2 category (Fig. 7). Note that it would only take a small portion of collagen fibrils linked in series to have a dramatic effect on the stiffness of the tissue because the tensile strength of collagen fibrils is quite high and the collagen fibrils would now be transferring stress more directly under tension as opposed to transferring it through a fluid. A small decrease in s_1 could, therefore, provide a large increase in s_2 (Fig. 7B), where s_2 represents the combined elastic properties of all elements that span the tissue specimen, including the microfibrillar network and any network formed by the linkage of collagen fibrils.

Changing the viscosity (d_1) in our model leads to interesting behavior defined by both positive and negative slopes (Fig. 6B) depending on the magnitude of the viscosity in relation to the spring constants. This ambiguity makes interpretation of the viscous contribution to stiffness difficult, especially as very little work has been performed to characterize the components of the dermis that are most likely to be responsible for the loss modulus of the tissue. There are several studies that refer to the 'viscosity' of a tissue (Eylers, 1982; Motokawa, 1984b; Motokawa and Hayashi, 1987; Trotter et al., 1997; Birenheide et al., 1998), but these address neither the viscosity of the fluid in the tissue nor the viscous constant in a theoretical model; instead, they refer to the resistance to flow of the entire tissue specimen, which can be easily altered by changes in any one of the three elements in our model.

The parabolic nature of the response of the model to a changing damping element prevents us from ruling out the possibility of a viscously driven stiffness change (see hypothetical mechanism 1 in the Introduction). However, this situation seems less likely than an elastically driven stiffening mechanism for three reasons. (i) Our data are well matched to the function produced by changing the s_2 elastic element, while only match one side of the function produced by changing d_1. (ii) Our data maintain a steady negative slope over several orders of magnitude, which is consistent with the function produced by changing the s_2 elastic element. Changing d_1 in the model results in a parabolic function with a negatively sloping region, but this becomes extremely steep after only a few-fold increase in stiffness, which is not seen in our data (note that, while the absolute values on the abscissa are arbitrary, the relative scale over which they occur is accurate). (iii) The changing s_2 mechanism has a simple explanation for which there is already evidence (that elastic elements can be linked by a molecule such as 'stiparin'; Trotter et al., 1997).

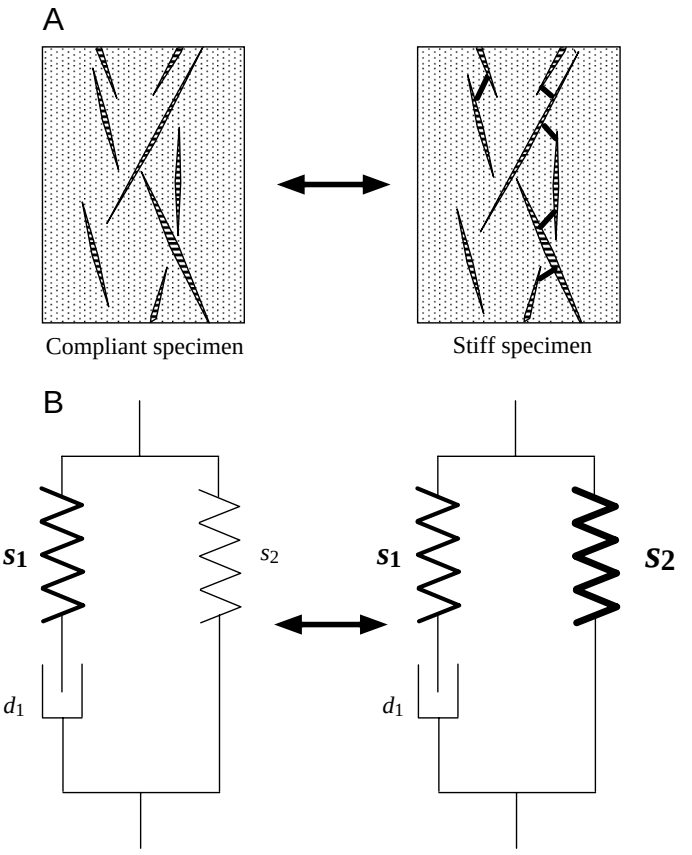

Fig. 7. Explanation for tissue stiffening. (A) Collagen fibrils within a tissue specimen link together to form a more continuous network (the microfibrils are not represented here). (B) A representation of such a change using the viscoelastic model. Fibrils accounted for by s_1 become part of s_2 as they form a continuous network. Note that only a small proportion of the collagen fibrils need to span the tissue to achieve a dramatic increase in stiffness; therefore, s_1 remains nearly the same while s_2 increases sharply. See Fig. 6 for an explanation of s_1, s_2 and d_1.

The mechanism by which an elastic network seems to be created and broken down, according to our model, is unknown. It seems most plausible to us that collagen fibrils are being linked together by some intermediate molecules or structures. Trotter et al. (1997) have shown that a proteinaceous tissue component that they call 'stiparin' flocculates isolated collagen fibrils in solution. Stiparin and other matrix molecules may be interacting with components released from cells to link collagen fibrils or their associated surface molecules *in vivo*. There is also the possibility that the microfibrillar network is involved in stiffening. This network was too weak to account for dermal stiffening when it was isolated from the rest of the

tissue *via* digestion (Thurmond and Trotter, 1996), but the extensiveness of its permeation in live tissue has not been documented.

In conclusion, this study has shown that crude inner and outer dermis extracts from *Cucumaria frondosa* produced stiff and compliant states respectively. Furthermore, they did so in a consistent fashion with regards to stiffness (G^*) and damping ($\tan\delta$) (equation 7), suggesting that the effects of the extracts are within the bounds of physiological relevance. If the tissue is modeled as a standard linear solid, the negative slope of the relationship between G^* and $\tan\delta$ supports a hypothetical stiffening mechanism wherein tissue components link with each other as the tissue stiffens. Our model suggests these linkages probably involve discontinuous collagen fibrils, but the details of the mechanism(s) for this remain enigmatic. These results markedly narrow the spectrum of hypotheses accounting for stiffening and can thus act as a guide for future research.

We would like to thank Peter Collins (Coastside Research, Stonington, ME, USA) for generously supplying *C. frondosa* specimens, the laboratory of Dr John Trotter for collaborative efforts and training in biochemistry, Dr Shyril O'Steen for help with statistical analysis and Dr Steve Katz, Dr Jennifer Nauen, Dr Torre Knower, H. Scott Rapoport and Dr John Gosline for helpful review and comments. This work was partially supported by NSF Grant DCB-9019284, Scripps Institution of Oceanography Graduate Department and Sigma Xi.

References

Birenheide, B., Tamori, M., Motokawa, T., Ohtani, M., Iwakoshi, E., Muneoka, Y., Fujita, T., Minakata, H. and Nomoto, K. (1998). Peptides controlling stiffness of connective tissue in sea cucumbers. *Biol. Bull.* **194**, 253–259.

Diab, M. and Gilly, W. F. (1984). Mechanical properties and control of non-muscular catch in spine ligaments of the sea urchin, *Strongelocentrotus franciscanus. J. Exp. Biol.* **111**, 155–170.

Eylers, J. (1982). Ion-dependent viscosity of holothurian body wall and its implications for the functional morphology of echinoderms. *J. Exp. Biol.* **99**, 1–8.

Eylers, J. P. and Greenberg, A. R. (1988). Mechno-chemistry of the cation sensitive cross-links in the catch connective tissue of holothurian body wall. In *Echinoderm Biology* (ed. R. D. Burke, P. V. Mladenov, P. Lambert and R. L. Parsley), pp. 629–634. Rotterdam: Balkema.

Eylers, J. and Greenberg, A. R. (1989). Swelling behavior of the catch connective tissue in holothurian body wall. *J. Exp. Biol.* **143**, 71–86.

Harris, B. (1980). The mechanical behavior of composite materials. In *The Mechanical Properties of Biological Materials* (ed. J. F. V. Vincent and J. D. Current), pp. 37–74. Cambridge: Cambridge University Press.

Hayashi, Y. and Motokawa, T. (1986). Effects of ionic environment on viscosity of catch connective tissue in holothurian body wall. *J. Exp. Biol.* **125**, 71–84.

Hidaka, M. and Takahashi, K. (1983). Fine structure and mechanical properties of the catch apparatus of the sea-urchin spine, a collagenous connective tissue with muscle-like holding capacity. *J. Exp. Biol.* **103**, 1–14.

Hyman, L. H. (1955). *The Invertebrates: Echinodermata*. New York: McGraw-Hill.

Kariya, Y., Watabe, S., Ochiai, Y. and Hashimoto, K. (1990). Glycosaminoglycan involved in the cation-induced change of body wall structure of the sea cucumber *Stichopus japonicus*. *Connect. Tissue Res.* **25**, 149–159.

Koob, T. J., Koob-Emunds, M. M. and Trotter, J. A. (1999). Cell-derived stiffening and plasticizing factors in sea cucumber (*Cucumaria frondosa*) dermis. *J. Exp. Biol.* **202**, 2291–2301.

Koob-Emunds, M., Trotter, J. and Koob, T. (1996). Identification of stiffening and plasticizing factors in sea cucumber (*Cucumaria frondosa*) dermis. *Bull. Mt Desert Island Biol. Lab.* **35**, 101–104.

Koob-Emunds, M., Trotter, J. and Koob, T. (1998). Segregation of stiffening and plasticizing factors in the dermis of *Cucumaria frondosa. Bull. Mt Desert Island Biol. Lab*. **37**, 120–122.

Motokawa, T. (1981). The stiffness change of the holothurian dermis caused by chemical and electrical stimulation. *Comp. Biochem. Physiol.* **70**C, 41–48.

Motokawa, T. (1982). Factors regulating the mechanical properties of holothurian dermis. *J. Exp. Biol.* **99**, 29–41.

Motokawa, T. (1984a). Connective tissue catch in echinoderms. *Biol. Rev.* **59**, 255–270.

Motokawa, T. (1984b). Viscoelasticity of the holothurian body wall. *J. Exp. Biol.* **109**, 63–75.

Motokawa, T. (1988). Catch connective tissues: A key character for echinoderm's success. In *Echinoderm Biology* (ed. R. D. Burke, P. V. Mladenov, P. Lambert and R. L. Parsley), pp. 39–54. Rotterdam: Balkema.

Motokawa, T. (1994). Effects of ionic environment on viscosity of Triton-extracted catch connective tissue of a sea cucumber body wall. *Comp. Biochem. Physiol.* **109**B, 613–622.

Motokawa, T. and Hayashi, Y. (1987). Calcium dependence of viscosity change caused by cations in holothurian catch connective tissue. *Comp. Biochem. Physiol.* **87**A, 579–582.

Scott, J. E. (1988). Proteoglycan–fibrillar collagen interactions. *Biochem. J.* **252**, 313–323.

Scott, J. E. (1991). Proteoglycan:collagen interactions in connective tissues. Ultrastructural, biochemical, functional and evolutionary aspects. *Int. J. Biol. Macromol.* **13**, 157–161.

Shadwick, R. E. and Pollock, C. (1988). Dynamic mechanical properties of sea urchin spine ligaments. In *Echinoderm Biology* (ed. R. D. Burke, P. V. Mladenov, P. Lambert and R. L. Parsley), pp. 635–640. Rotterdam: Balkema.

Shibayama, R., Kobayashi, T., Wada, H., Ushitani, H., Inoue, J., Kawakami, T. and Sugi, H. (1994). Stiffness changes in holothurian dermis induced by mechanical vibration. *Zool. Sci.* **11**, 511–515.

Smith, D. S., Wainwright, S. A., Baker, J. and Cayer, M. L. (1981). Structural features associated with movements and 'catch' of sea-urchin spines. *Tissue & Cell* **13**, 299–320.

Szulgit, G. K. and Shadwick, R. E. (1994). The effects of calcium chelation and cell perforation on the mechanical properties of sea urchin ligaments. In *Echinoderms Through Time: Proceedings of the Eighth International Echinoderm Conference* (ed. B. David), pp. 887–892. Rotterdam: A. A. Balkema.

Szulgit, G. K. and Shadwick, R. E. (1998). Novel non-cellular adhesion and tissue grafting in the mutable collagenous tissue of

the sea cucumber *Parastichopus parvimensis*. *J. Exp. Biol.* **201**, 3003–3013.

Takahashi, K. (1967). The ball-and-socket joint of the sea-urchin spine: geometry and its functional implications. *J. Fac. Sci. Univ. Tokyo IV* **11**, 131–135.

Thurmond, F. A. and Trotter, J. A. (1996). Morphology and biomechanics of the microfibrillar network of sea cucumber dermis. *J. Exp. Biol.* **199**, 1817–1828.

Trotter, J. A., Chapman, J. A., Kadler, K. E. and Holmes, D. F. (1998). Growth of sea cucumber collagen fibrils occurs at the tips and centers in a coordinated manner. *J. Mol. Biol.* **284**, 1417–1424.

Trotter, J. A. and Koob, T. J. (1995). Evidence that calcium-dependent cellular processes are involved in the stiffening response of holothurian dermis and that dermal cells contain an organic stiffening factor. *J. Exp. Biol.* **198**, 1951–1961.

Trotter, J. A., Lyons-Levy, G., Thurmond, F. A. and Koob, T. J. (1995). Covalent composition of collagen fibrils from the dermis of the sea cucumber, *Cucumaria frondosa*, a tissue with mutable mechanical properties. *Comp. Biochem. Physiol.* **112**A, 463–478.

Trotter, J., Salgado, J. and Koob, T. (1997). Mineral content and salt-dependent viscosity in the dermis of the sea cucumber *Cucumaria frondosa*. *Comp. Biochem. Physiol.* **116**A, 329–335.

Trotter, J. A., Thurmond, F. A. and Koob, T. J. (1994). Molecular structure and functional morphology of echinoderm collagen fibrils. *Cell Tissue Res.* **258**, 451–458.

Ward, I. M. (1983). *Mechanical Properties of Solid Polymers*, 2nd edn. Chichester: John Wiley & Sons. 475pp.

Wilkie, I. C. (1978). Nervously mediated change in the mechanical properties of a brittlestar ligament. *Mar. Behav. Physiol.* **5**, 289–306.

Wilkie, I. C. (1984). Variable tensility in echinoderm collagenous tissues: a review. *Mar. Behav. Physiol.* **11**, 1–34.

Wilkie, I. C. (1996). Mutable collagenous tissues: Extracellular matrix as mechano-effector. *Echinoderm Studies* **5**, 61–102.

Wilkie, I. C. and Emson, R. H. (1988). Mutable collagenous tissues and their significance for echinoderm paleontology and phylogeny. In *Echinoderm Phylogeny and Evolutionary Biology* (ed. C. R. C. Paul and A. B. Smith), pp. 311–330. Oxford: Clarendon Press.